ANL/PHY/CP--87762
CONF-9509125--13

Time Evolution of Charge States in an ECR Ion Source

R.C. Pardo, R. Harkewicz*, and P.J. Billquist
Argonne National Laboratory

Abstract

The production of high charge-state ions in an ECR ion source has been studied as a function of time using a pulsed NdYAG laser to ablate heavy metal (bismuth) ions into the plasma. The time required to produce a charge state has been measured by observing the arrival time of the ions at a Faraday cup after the source analyzing magnet. The results of these measurements have been compared to a simple sequential ionization model and are found to be in good agreement with the data. The data can be used to characterize the plasma electron density, electron temperature and neutral atom density since these are the only three adjustable parameters in the model and are sufficient to achieve good agreement for the time evolution of all observed charge states.

*Present address: National Superconducting Cyclotron Laboratory, Michigan State University, East Lansing, MI

Introduction

The time dependence for the production of specific charge-state ions in an electron cyclotron resonance (ECR) ion source has been studied as part of an overall program to investigate the feasibility of using laser ablation to dope an ECR plasma with solid material ions and produce beams of interest from these ions. We have been able to measure the creation and the subsequent decay of individual charge states in the plasma and follow the progression of those ions to higher and higher charge states by observing their time-dependent loss from the source. Although these measurements are actually carried out in sequential steps, they constitute the first direct measurement of the confinement time for ions in an ECR ion source and an unambiguous demonstration of the dominance of sequential ionization and charge exchange recombination in the formation of these ions.

A very simple model including only single-electron stripping and recombination events has been created to attempt to understand the results of our measurements. Within the context of this simple model, containing only three parameters, nearly all the features of the time profile of each charge state studied has been reproduced. The strong interplay between neutral plasma density and electron temperature is strongly demonstrated.

Experimental Setup and Results

The Argonne PIIECR[1] ion source, shown in cross-section in figure 1, was developed with an effort to make the production of beams from normally solid materials as versatile and easy as possible. Four narrow radial ports exist which allow direct access for materials to be inserted into or near the plasma. The four-fold symmetry of the configuration creates a port 180° opposite any other port and provides the opportunity to irradiate a sample with a high-power laser to ablate material directly into the source.

The laser used is a Q-switched NdYAG laser operating at 1064 nm. The Q-switch can be operated at repetition rates from DC to approximately 1 kHz without loss of pulse energy. In this mode, the laser generates pulses of approximately 200 ns width with peak energy densities of 10^7 watts/ cm^2. This is not sufficient power to expect significant ablation of most materials of interest, but it is sufficient to demonstrate the ability of this technique for solid material insertion. Because of the laser's low power, we were required to use materials which could be easily evaporated with our laser. Bismuth is an excellent example of such a material and was chosen for these tests.

The optical path used was very simple, dictated by the existing geometry of the source, and is shown schematically in Figure 1 and to scale in Figure 2. The laser was mounted on an adjacent wall as was a 90° mirror. On the source entrance window, a lens was separately mounted and adjusted to produce a focus at the bismuth target location.

The laser shines through the window, across the plasma, and onto the bismuth sample. Bismuth evaporates/ablates from the sample and recoils into the plasma where it is ionized.

The short beamline from the source to the Faraday Cup measurement point is shown in Figure 2. The total path length is 2.5 meters. The flight time for the slowest ion studied is approximately 1.4 μsec. This delay is short compared to the observed productions time and was ignored in the subsequent analysis.

The model for laser ablation is that the ions on the surface, only one or two wavelengths deep, are heated 'instantaneously' by the laser to sufficient temperatures to evaporate or recoil from the surface. The intention of the extremely high power, short pulse, is to deliver all the power on a time scale so short that conductive processes cannot remove significant energy from the target region and much of the energy goes into atom removal. We only require this model to be sufficiently true as to be able to ignore any evaporation time scales and claim that the ion injection time is short compared to any ionization time measured in these experiments. All time scales involving evaporation and transit time from sample to plasma are on the order of one microsecond, or shorter, compared to the millisecond time scales which are presented below. Therefore we assume that the injection into the plasma occurs instantaneously in all subsequent discussions.

The source was tuned on oxygen support gas and then the laser was operated and a bismuth charge state spectrum was observed and tuned. At that point a resistor of 1 MΩ was placed in the output of the Faraday cup and the voltage pulse generated across the resistor was viewed on an oscilloscope. Because of the long time scales observed in these measurements, concerns about impedance matching were of no importance as can be seem from the figures presented below.

Individual charge states, 10+ through 24+, were then selected by the analyzing magnet and the laser was operated on a very slow pulse repetition rate of one Hertz. The time structure of the arriving ions at the Faraday cup was then observed for the selected charge state and photographed. The data photographs are shown in Figure 3 for the charge states which could be cleanly studied.

The first feature we noted in the data was the very precise evolution of the peak in the ion distributions to longer and longer times with increasing charge state. The steps are quite regular with, but not proportional to, charge state. The second feature of the data to be noted is the quite dramatic increase in the width of the time distribution with increasing charge state. This is true for both the 'rise' time and for the 'decay' time of the pulses, although the 'decay' time lengthens out significantly more than does the 'rise' time at higher charge states.

The last feature to note in the time distribution of ions is the small, fast pulse which is first visible in the time spectrum of the 20+ ions and increases significantly with increasing charge state. This feature is interpreted as the equivalent of the 'afterglow'[2] effect in pulsed ECR operation. That is, these ions are believed to be residual, confined ions in the plasma at the time the laser pulse occured and were expelled due to the plasma de-confinement created by the laser, or more likely, the large burst of neutral atoms injected into the plasma from the laser pulse. If so it is another, rather dramatic, confirmation of the preferential confinement of high charge-state ions in the plasma.

The photographs were analyzed by hand and eye and the position of the peak in the current distribution, the growth half-time and the decay half-time were extracted and are presented in Table I. The precision of these values is estimated to be ±10% or better.

Calculation Model

A model has been developed to assist in the understanding of these results. The first simple model assumed only sequential stripping of ions and followed the time evolution of charge states using only this process as the driving term. Such a model is too simple to hope to accurately reproduce many features. In such a model for example, there is no possibility to achieve equilibrium in the distribution. Even so the overall qualitative features of the data were quite well reproduced, especially for the lower charge states. This is not surprising since recombination rates are small for the lower charge states in the region of parameter space in which ECR plasmas are expected to exist.

This model was then made somewhat more realistic by including the recombination charge exchange process. Radiative and dielectronic recombination have been ignored since their rates are significantly below those of the charge exchange process in the ECR environment. A set of thirty differential equations were solved simultaneously to determine the time evolution of each charge state. Each equation had the form:

$$\frac{dN_i}{dt} = \lambda_{i-1} N_{i-1}(t) - (\lambda_i + \nu_i) N_i(t) + \nu_{i+1} N_{i+1}(t) \qquad (1)$$

where N_i is the number of ions of charge-state i, λ_i is the stripping reaction rate for ions of charge i to strip to $i+1$, and ν_i is the reaction rate for ions of charge i to charge-exchange back to charge $i-1$.

The stripping rate is the velocity-averaged rate assuming a Boltzmann distribution characterized by an electron temperature, T_e, and electron density, n_e. This rate is given by[3]:

$$\lambda_i = \left(\frac{2}{\sqrt{\pi}}\right)\int \sigma_{ion} v n_e \left(\frac{E_e^{1/2}}{T_e^{3/2}}\right) e^{-\frac{E_e}{T_e}} dE_e \qquad (2),$$

integrated over the electron energy, E_e. The cross-section, σ_{ion}, is taken from the formulae given by Lotz[4] while the necessary ionization potentials come from Carlson[5]

The charge-exchange rate is the ion thermally averaged cross section using the cross-section formula by Müller and Salzborn[6]. West[3] shows the thermally averaged result for ions of charge state Q_i, mass A, and thermal temperature T_{ion} to be:

$$\nu_i = 3.15(-6) n_{npl} Q_i^{1.17} P_{0\to 1}^{-2.75} \sqrt{\frac{T_{ion}}{A}} \qquad (3)$$

where n_{npl} is the neutral ion density and $P_{0\to 1}$ is the neutral atom first ionization potential.

For the simplest model where the charge-exchange recombination was ignored, analytic solutions to the differential equations could be found and the time dependent number densities analytically evaluated after performing the integral of equation 2. For the more complex equations including charge exchange, the equations were evaluated numerically using the program Mathcad[7]. These two approaches agreed when all charge-exchange rates were set to zero, giving a cross check on the results.

In this simple model there are three free parameters which can be adjusted in an attempt to reproduce the data in Table I. Those free parameters are the electron density and temperature, n_e and T_e, and the neutral density, n_{npl}. Cases were calculated in an effort to select the best fit to the data and to determine the sensitivity to these three parameters.

The results of the calculations are shown in Table II for a selected set of charge states and for the parameters sets which gave good agreement with the data. The calculated time evolution of some selected charge states is shown graphically in Figure 4 for the case corresponding to column five in Table II. We find that different features in the spectra limit the acceptable ranges for the three free parameters of the fit. Electron density, n_e, is strongly limited by the low charge state distribution peaks as well as the low charge-state rise and decay times and is has only a weak dependence on T_e and n_{npl}. The range of n_e which give reasonable fits to the data is $4X10^{11}$ to $6X10^{11}$. The value of the parameters of electron temperature, T_e, and neutral density, n_{npl}, are largely set by the high charge state distribution peaks and by the high charge-state rise time, respectively. This separation of dependence can also be seen in the more elaborate model of Shirkov, et al[8]. These two parameters are somewhat more coupled to each other, are not as well determined as the electron density, and are much more model dependent. Acceptable agreement with the data is possible for T_e between 1500 and 4000 eV and for n_{npl} between $2.0X10^9$ to $3.3X10^{10}$. Significant discrepancies with the data exist outside these parameter ranges.

The most poorly reproduced parameters were the decay times for the high charge state ions (20+ and 24+ in Table II). A reasonable case can be made that the decay times of these highest charge states should not be reproduced by this simple model since a significant portion of the decay of these charge states will be due to the escape from the source of these equilibrium ions. No attempt was made to include this channel which actually gave rise to the data on which these measurements are based. The lower charge states which are rapidly being depleted by population of the higher ionization states are not effected by this omission, but the charge states around the middle twenties are the ones predicted to be the equilibrium charge states and their loss only occurs by the depletion of ions from the plasma. The prediction of equilibrium onset is shown in Figure 4 for the case corresponding to column 4 in Table II. If we relax the desire to fit the fall times for the high charge states, then the parameter set shown in column 4 of Table II is the best fit obtained for the data and is in good agreement with the expectation of neutral plasma density for the operated source configuration. The parameter set then requires a neutral plasma density which predicts an equilibrium charge state distribution and shows that equilibrium is obtained in approximately 100 milliseconds. The required electron temperature for this case is also approximately 2 times the temperature needed when a very low neutral plasma density is required.

Within this simple model the parameters of electron density, electron temperature, and neutral plasma density are rather well constrained. Within the model used, the important interplay between neutral pressure and electron temperature is made very apparent. The calculations show that the time evolution of charge states is quite sensitive to plasma parameters and could be used as an important tool to better understand ECR plasmas. A more elaborate model applied to data such as presented here would be quite interesting and beneficial in improving our understanding of the most desirable parameter ranges for high charge state production in ECR ion sources.

This work was supported by US D.O.E. Nuclear Physics Division under contract W-31-1-0-ENG-38.

Table I. Bismuth Charge-State Time Dependence Parameters

Charge State (Q)	Q-Peak Time (msec.)	Growth Half-life (msec.)	Decay Half-life (msec.)
10	2.5	1.2	1.6
11	3.1	1.6	2.9
12	4.2	2.5	2.9
14	5.3	2.9	3.9
16	6.9	3.7	5.0
17	9.3	4.0	5.6
18	9.9	5.0	8.1
19	13.4	6.4	9.9
20	15.5	8.1	16.5
21	19.0	10.8	16.9
22	25.0	12.0	21.5
23	31.0	17.4	33.0
24	37.5	23.2	41.0

Table II. Calculated Results Compared to Data for Selected Charge States

Electron Den. (cm^{-3}) Electron Temp (eV) Neut. Den (cm^{-3})	Experiment Experiment Experiment	$5X10^{11}$ 1500 $2.2X10^{9}$	$5X10^{11}$ 2000 $4.4X10^{9}$	$5X10^{11}$ 4000 $3.3X10^{10}$
10+ peak (msec)	2.5	2.7	2.6	2.6
10+ rise (msec)	1.3	1.0	1.0	1.0
10+ fall (msec)	2.6	1.2	1.3	0.9
16+ peak (msec)	6.9	8.9	8.2	8.0
16+ rise (msec)	3.2	3.0	2.7	2.8
16+ fall (msec)	5.0	4.2	3.7	5.1
20+ peak (msec)	15.5	18.3	16.3	18.6
20+ rise (msec)	7.4	5.8	6.2	7.7
20+ fall (msec)	16.5	8.0	7.6	32.9
24+ peak (msec)	37.2	36.2	32.1	36
24+ rise (msec)	14.3	11.3	10.4	14.5
24+ fall (msec)	41.0	17.8	16.7	none

Figure Captions.

Figure 1. Cross-section of the source, sample, and laser path geometry used.

Figure 2. Floor plan showing the physical relationship of the source, laser, beamine, and Faraday cup detector used.

Figure 3. A sequence of oscilloscope trace photographs of the detected beam current at the Faraday cup as a function of time for each charge state investigated.

Figure 4. Calculated time evolution of selected charge states for the plasma parameters corresponding to the last column in Table II.

References

[1] R. Pardo, Nucl. Instrum. and Meth. Phys. Res., **B40/41**, 1014(1989).
[2] P. Sortais, Rev. Sci. Instrum., **63**(4), 2801(1992).
[3] H. I. West, Jr. Lawrence Livermore National Laboratory Report UCRL-53391, 1982.
[4] W. Lotz, Z. Physik, **216**, 241(1968).
[5] T.A. Carlson, C.W. Nestor, Jr., N. Wasserman, and J.D. McDowell, Atomic Data, **2**, 63(1970).
[6] A. Müller and E. Salzborn, Physics Letters, **62A**, 391(1977).
[7] Mathcad Plus 5.0, MathSoft, Inc., 101 Main St., Cambridge, MA 02142.
[8] G. D. Shirkov, C. Mühle, G. Musiol, and G. Zschornack, Nulc. Instrum. & Meth., **A302**, 1(1991).

ANL-P-21,500

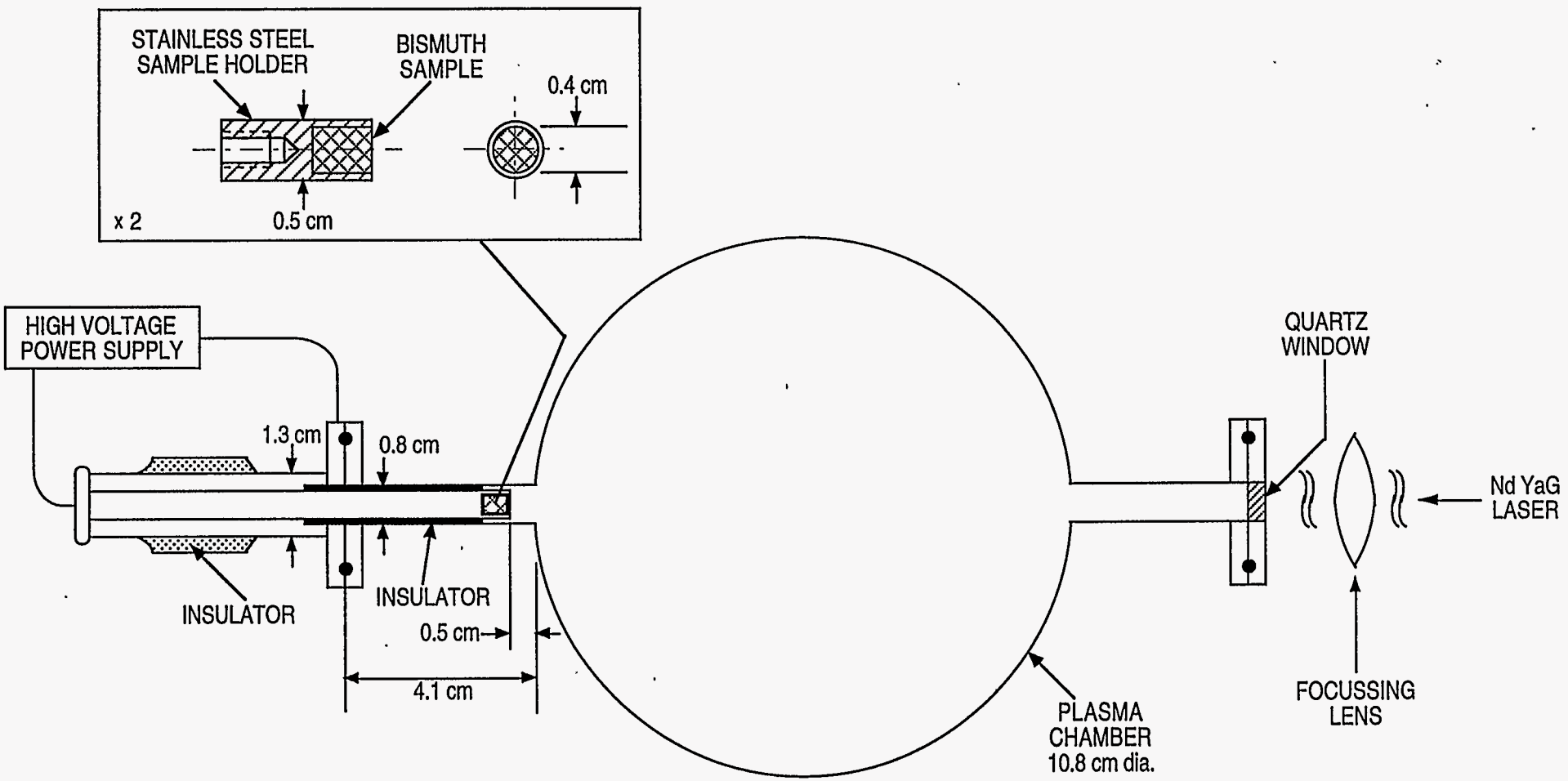
STAINLESS STEEL SAMPLE HOLDER
BISMUTH SAMPLE
0.4 cm
x 2
0.5 cm
HIGH VOLTAGE POWER SUPPLY
1.3 cm
0.8 cm
INSULATOR
INSULATOR
0.5 cm
4.1 cm
QUARTZ WINDOW
Nd YaG LASER
FOCUSSING LENS
PLASMA CHAMBER 10.8 cm dia.

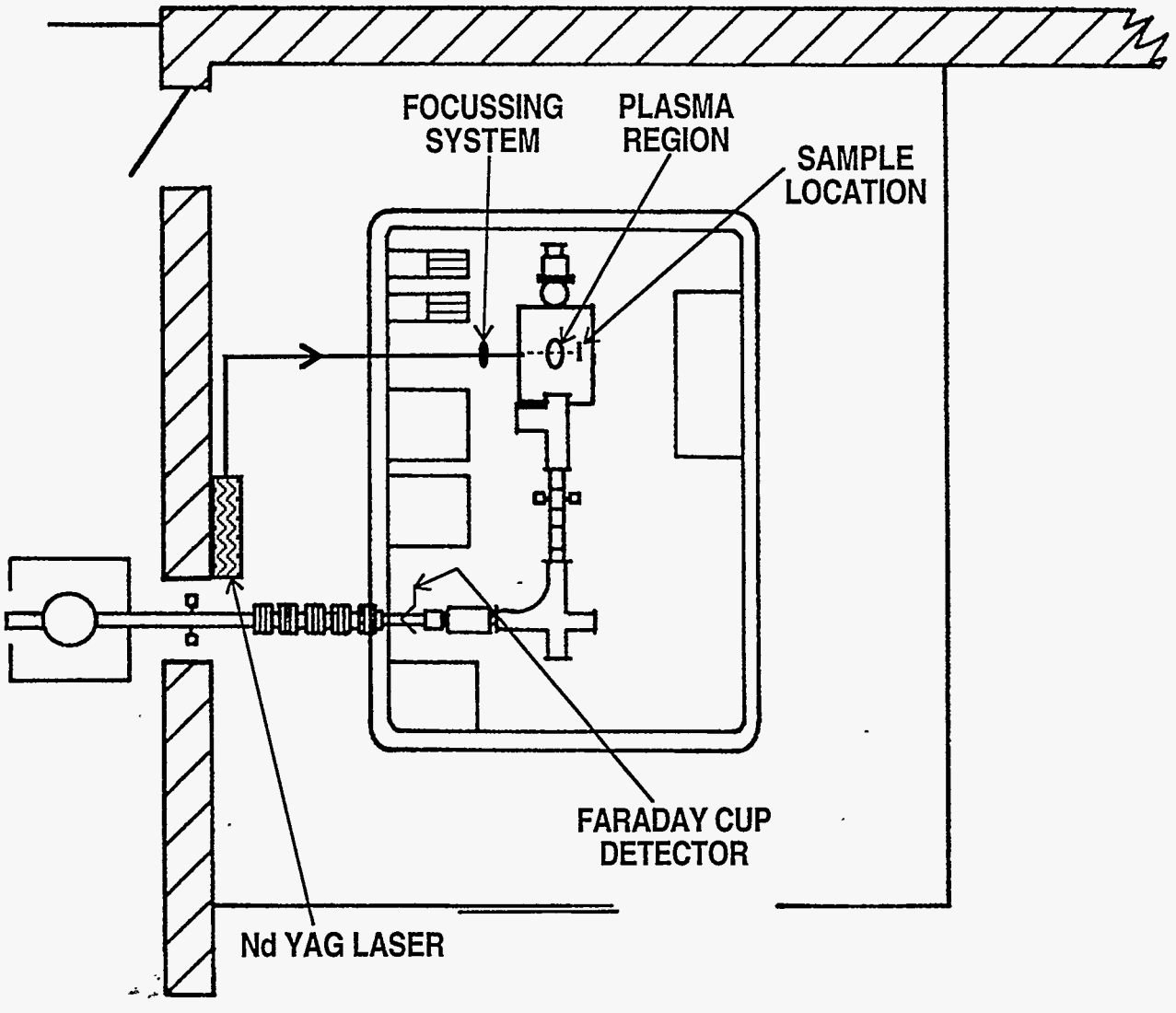
FOCUSSING SYSTEM
PLASMA REGION
SAMPLE LOCATION
FARADAY CUP DETECTOR
Nd YAG LASER

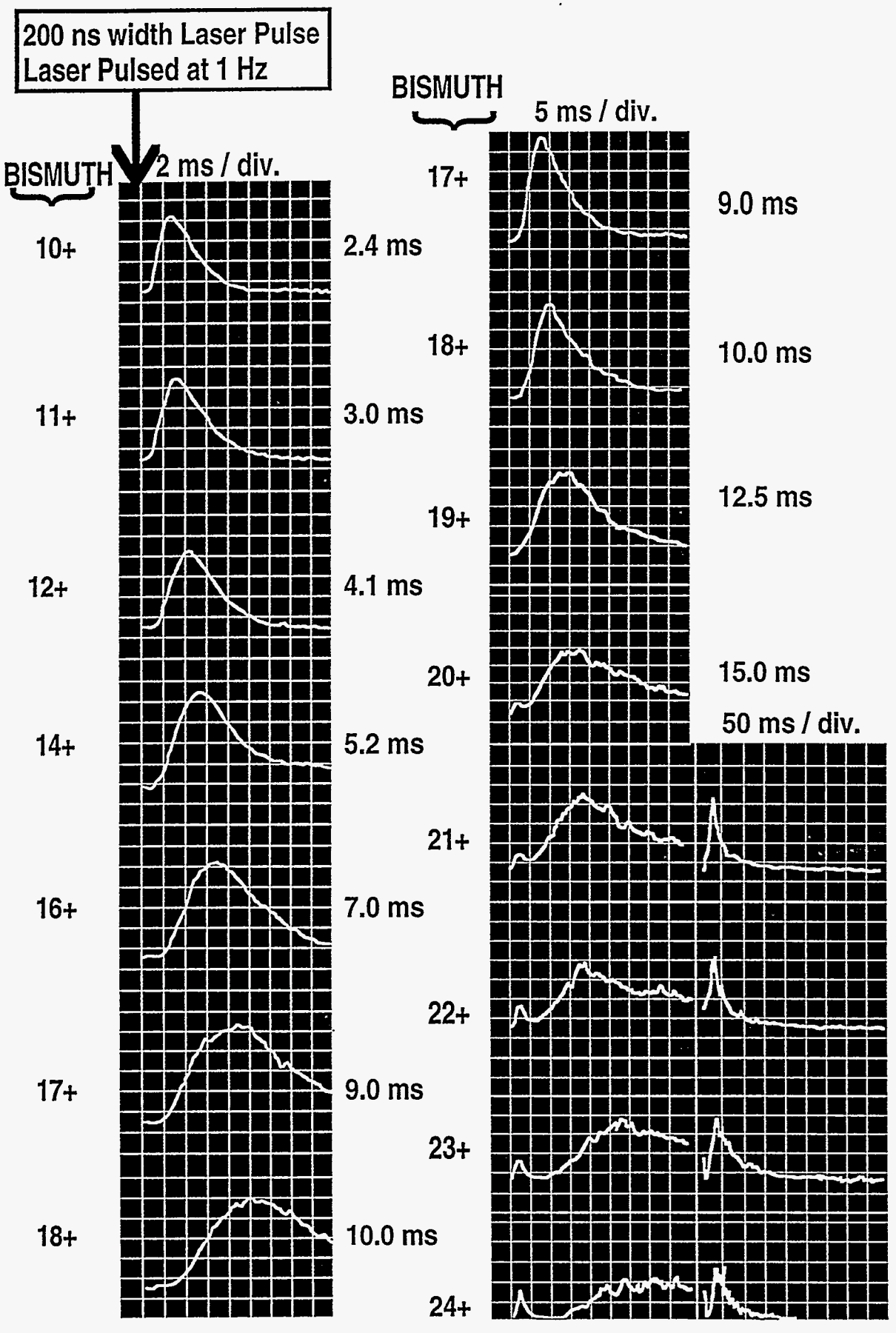
200 ns width Laser Pulse
Laser Pulsed at 1 Hz
BISMUTH
2 ms / div.
10+
2.4 ms
11+
3.0 ms
12+
4.1 ms
14+
5.2 ms
16+
7.0 ms
17+
9.0 ms
18+
10.0 ms
BISMUTH
5 ms / div.
17+
9.0 ms
18+
10.0 ms
19+
12.5 ms
20+
15.0 ms
50 ms / div.
21+
22+
23+
24+

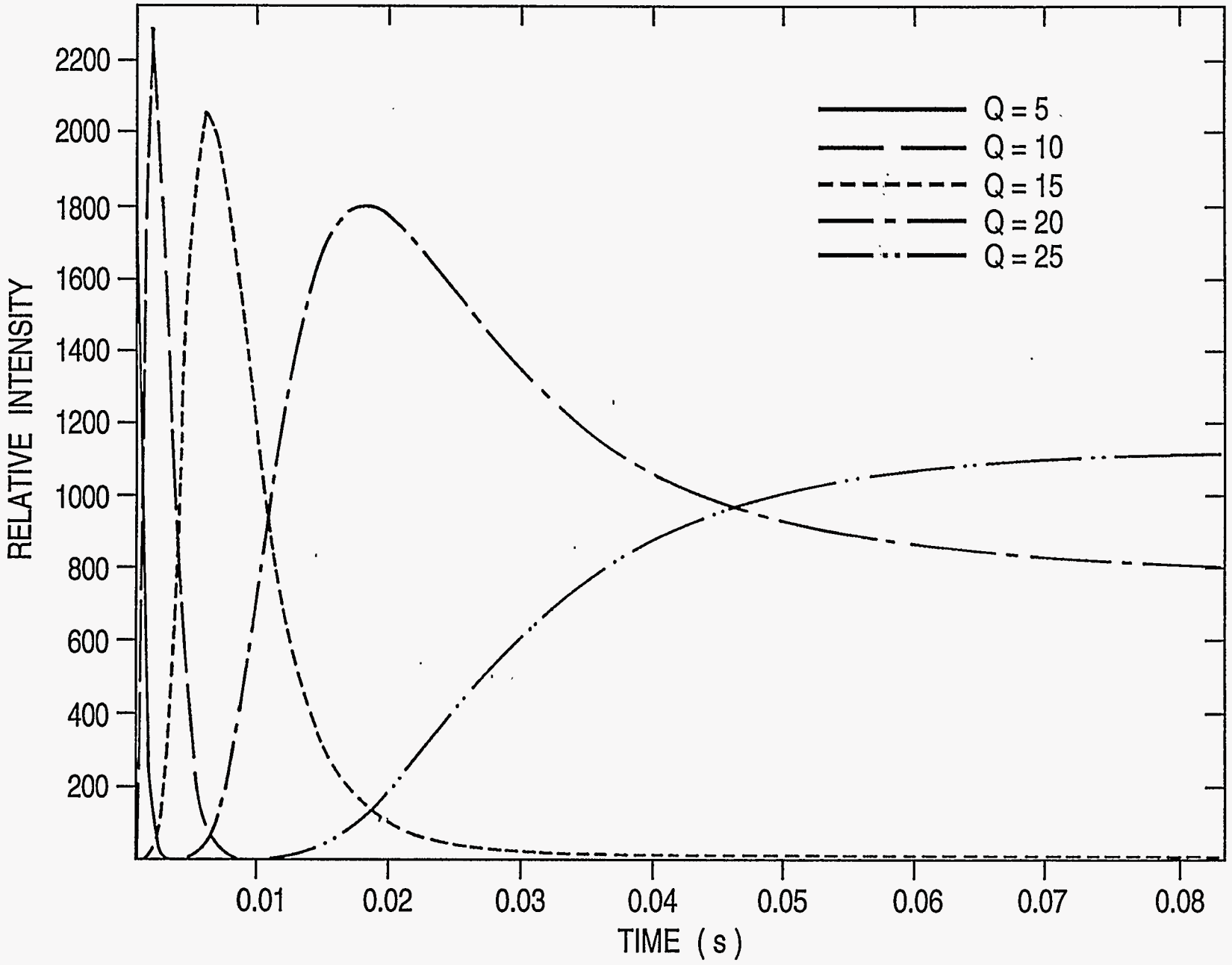
RELATIVE INTENSITY
2200
2000
1800
1600
1400
1200
1000
800
600
400
200
0.01
0.02
0.03
0.04
0.05
0.06
0.07
0.08
TIME (s)
Q = 5
Q = 10
Q = 15
Q = 20
Q = 25